Available online at www.sciencedirect.com
SCIENCE DIRECT
Journal of Computational Physics 214 (2006) 1–11
JOURNAL OF COMPUTATIONAL PHYSICS
www.elsevier.com/locate/jcp

Short note

A high-order Padé ADI method for unsteady convection–diffusion equations

Donghyun You *

Center for Turbulence Research, Stanford University, 488 Escondido Mall, Building 500, Room 500X, Stanford, CA 94305, USA

Received 12 July 2005; received in revised form 5 October 2005; accepted 6 October 2005
Available online 22 November 2005

Abstract

A high-order alternating direction implicit (ADI) method for computations of unsteady convection–diffusion equations is proposed. By using fourth-order Padé schemes for spatial derivatives, the present scheme is fourth-order accurate in space and second-order accurate in time. The solution procedure consists of a number of tridiagonal matrix operations which make the computation cost effective. The method is unconditionally stable, and shows higher accuracy and better phase and amplitude error characteristics than the standard second-order ADI method [D.W. Peaceman, H.H. Rachford Jr., The numerical solution of parabolic and elliptic differential equations, Journal of the Society of Industrial and Applied Mathematics 3 (1959) 28–41] and the fourth-order ADI scheme of Karaa and Zhang [High order ADI method for solving unsteady convection–diffusion problem, Journal of Computational Physics 198 (2004) 1–9].

Keywords: Unsteady convection–diffusion equation; High order scheme; Padé scheme; ADI method; Finite difference method

1. Introduction

The unsteady convection–diffusion equation for a variable ϕ in two-dimensional space can be written as

$$\begin{aligned}
&\frac{\partial \phi}{\partial t} = -c^x \frac{\partial \phi}{\partial x} - c^y \frac{\partial \phi}{\partial y} + v^x \frac{\partial^2 \phi}{\partial x^2} + v^y \frac{\partial^2 \phi}{\partial y^2}, \quad (x,y) \in \Omega \times (0,T], \\
&\phi(0,x,y) = \phi_0(x,y), \quad (x,y) \in \Omega, \\
&a(t,x,y)\phi + b(t,x,y)\frac{\partial \phi}{\partial n} = f(t,x,y), \quad (x,y) \in \partial\Omega, \ \ t \in (0,T],
\end{aligned} \tag{1}$$

where $\Omega \subset \mathbb{R}^2$ is a rectangular domain, $(0,T]$ is the time interval, and ϕ_0 and f are the initial and boundary conditions. a and b are arbitrary coefficients describing the boundary condition as a Dirichlet, Neumann, or Robin type in the boundary normal direction n. $c^{x(y)}$ and $v^{x(y)}$ denote the convection velocity and viscosity

* Tel.: +1 650 725 1821; fax: +1 650 725 3525.
E-mail address: dyou@stanford.edu.

0021-9991/$ - see front matter © 2005 Elsevier Inc. All rights reserved.
doi:10.1016/j.jcp.2005.10.001

in the $x(y)$-direction, respectively. This equation is commonly encountered in physical sciences governing the transport of a quantity such as mass, momentum, heat, and energy.

Finite difference schemes have been widely used to solve the equation using combinations of various spatial and temporal discretization methods [1–9]. Among them, the alternating direction implicit (ADI) method proposed by Peaceman and Rachford [1] has been popular due to its computational cost-effectiveness. However, like other first- and second-order accuracy schemes, the Peaceman–Rachford ADI (PR-ADI) scheme, which is second-order accurate, often produces significant dissipation and phase errors, especially for convection-dominated problems [2]. In [7–9], iterative or non-iterative multistep methods were combined with the ADI method to achieve higher-order temporal accuracy.

To achieve higher spatial accuracy, recently, the high-order compact (HOC) scheme [10] has been utilized for spatial discretizations. This scheme leads to fourth-order accurate approximations. Furthermore, the HOC scheme produces non-oscillatory solutions for the steady homogeneous convection–diffusion equation [4]. Other classes of high-order compact schemes which have different weighting parameters have been derived by Rigal [5]. For solving unsteady convection–diffusion equations, the HOC scheme has been utilized in a number of different ways. Noye and Tan [6] developed a third-order nine-point HOC scheme for unsteady convection–diffusion equations, and later, Kalita et al. [3] increased the order of accuracy to fourth-order using the same bandwidth of stencil. The ADI approach was not employed in those methods, and therefore, computational costs were significantly higher than that of the PR-ADI method. The computational efficiency of the ADI approach and high-order accuracy of the HOC scheme were combined in the method proposed by Karaa and Zhang [2]. The high-order compact ADI (HOC-ADI) scheme retains the tridiagonal algorithm of the standard ADI [1], and at the same time, achieves fourth-order accuracy in space.

Although a number of test problems at relatively low cell Reynolds numbers ($Pe = c^{x(y)}h_{x(y)}/v^{x(y)}$, where $h_{x(y)}$ is the grid spacing) were considered in the HOC-based schemes [2,3,6], interestingly, the characteristics of the schemes at high cell Reynolds numbers and the resulting numerical errors in terms of phase and amplitude were not discussed. Many fully implicit and semi-implicit algorithms for solving Navier–Stokes equations also utilize the computational effectiveness of the ADI-type approach (e.g. [11–14]). Therefore, Navier–Stokes solutions will be one of the most promising applications of ADI methods with high-order spatial accuracy. It is well known that, in turbulent flow computations using direct numerical simulation or large eddy simulation, numerical dissipation induced by artificial diffusion or by truncation errors of the numerical scheme significantly degrades the solution quality [15]. As will be shown in the present study, HOC-based schemes suffer from excessive numerical dissipation at high cell Reynolds numbers.

In this note, a Padé scheme-based ADI (PDE-ADI) method is proposed. The present scheme employs the standard fourth-order accurate approximations for first and second derivatives in the convection–diffusion equation, while retains second-order accuracy in time utilizing the efficiency of tridiagonal algorithms. Furthermore, in contrast to the HOC-based schemes in which the phase and amplitude characteristics of a solution are altered by the variation of cell Reynolds number, the present method retains the characteristics of the modified wave numbers for spatial derivatives regardless of the variation of cell Reynolds number.

The superiority of the proposed scheme compared to other ADI schemes [1,2] for solving unsteady convection–diffusion equations is discussed in detail.

2. High-order Padé ADI scheme

Applying the Crank–Nicolson scheme and the ADI factorization for time integration of Eq. (1) results in

$$\left\{1+\frac{\Delta t}{2}\left(c^x\frac{\partial}{\partial x}-v^x\frac{\partial^2}{\partial x^2}\right)\right\}\left\{1+\frac{\Delta t}{2}\left(c^y\frac{\partial}{\partial y}-v^y\frac{\partial^2}{\partial y^2}\right)\right\}\phi^{n+1} = \left\{1-\frac{\Delta t}{2}\left(c^x\frac{\partial}{\partial x}-v^x\frac{\partial^2}{\partial x^2}\right)\right\}\left\{1-\frac{\Delta t}{2}\left(c^y\frac{\partial}{\partial y}-v^y\frac{\partial^2}{\partial y^2}\right)\right\}\phi^n+\mathcal{O}(\Delta t^2). \tag{2}$$

In the HOC-based schemes [2–4,6], the convection–diffusion terms in each direction are approximated with fourth-order accuracy as follows:

$$\left(c^x\frac{\partial}{\partial x}-\nu^x\frac{\partial^2}{\partial x^2}\right)\phi=f^x, \tag{3}$$

$$c^x\delta_x\phi_i-\nu^x\left(1+\frac{Pe_x^2}{12}\right)\delta_x^2\phi_i=f_i^x+\frac{h_x^2}{12}\delta_x^2 f_i^x-\frac{Pe_x h_x}{12}\delta_x f_i^x, \tag{4}$$

where δ_x and δ_x^2 are the second-order central difference operators for first and second derivatives, respectively. HOC approximations as given in Eq. (4) are incorporated into the ADI factored Eq. (2) to complete the HOC-ADI scheme proposed by Karaa and Zhang [2]. This method is unconditionally stable and retains fourth-order accuracy in space and second-order accuracy in time. Also, the HOC-ADI scheme equipped with tridiagonal algorithms results in a significant computational cost saving compared to other non-ADI-based iterative HOC schemes [3,6] (see [2] for more details).

Two important observation can be made about Eq. (4). First, the cell Reynolds number is present in the stencil coefficients. This feature results in a non-oscillatory solution by adding numerical dissipation depending on the cell Reynolds number for the steady homogeneous convection–diffusion equation [4]. However, the non-oscillatory feature is not guaranteed in unsteady problems [4], and as will be shown in this note, the scheme produces significantly enhanced dissipation in cases of high cell Reynolds numbers. The other point is that the approximation becomes singular for pure convection problems ($\nu^x=0$), while for pure diffusion problems ($c^x=0$), the HOC approximation becomes the standard fourth-order Padé scheme.

To examine the characteristics of the HOC scheme in more detail, a modified wave number analysis of Eq. (3) is performed. The modified wave number analysis allows one to assess how well different frequency components of a harmonic function in a periodic domain are represented by a finite-difference scheme [16]. Replacing the difference operators in Eq. (4) with modified wave numbers for second-order central differences results in

$$\lambda_{\mathrm{HOC}}=\left(\mathrm{i}c^x k^1+\nu^x\left(1+\frac{Pe_x^2}{12}\right)k^2\right)\Big/\left(-\mathrm{i}\frac{Pe_x h_x}{12}k^1+1-\frac{h_x^2}{12}k^2\right). \tag{5}$$

For comparison, the standard second-order central difference (CD) and fourth-order Padé (PDE) approximations of Eq. (3) are also considered, for which

$$\lambda_{\mathrm{CD}}=\mathrm{i}c^x k^1+\nu^x k^2, \tag{6}$$

$$\lambda_{\mathrm{PDE}}=\mathrm{i}c^x\hat{k}^1+\nu^x\hat{k}^2, \tag{7}$$

where $k_1=\sin kh_x/h_x$, $k^2=(2-2\cos kh_x)/h_x^2$, $\hat{k}^1=3\sin kh_x/h_x(2+\cos kh_x)$ and $\hat{k}^2=12(1-\cos kh_x)/h_x^2(5+\cos kh_x)$.

Fig. 1 shows the real and imaginary parts of λs as functions of kh_x for two different cell Reynolds numbers. In the case of $Pe=0.1$, shown in Fig. 1(a), the real parts for both the HOC and Padé schemes are almost indistinguishable, while the Padé scheme shows better resolution than the HOC scheme in the imaginary parts of λ. Both schemes show better resolution properties than the second-order central difference scheme. However, if the cell Reynolds number is increased to 10, the HOC scheme dramatically increases dissipation error (Real(λ)) and produces a significant overshoot in the imaginary part of λ (see Fig. 1(b)). This suggests that the solution quality of the HOC scheme is highly dependent on the cell Reynolds number. Especially, at a high Reynolds number, significant numerical dissipation is expected which is undesirable in turbulent flow computations using direct numerical simulation or large eddy simulation [15].

In contrast to the HOC scheme, the Padé scheme-based algorithm does not alter its non-dissipative characteristics with the cell Reynolds number. However, the tridiagonal matrix algorithms are not retained if we apply the Padé approximations directly to Eq. (2). To overcome this deficiency, further factorizations are made without loss of temporal accuracy,

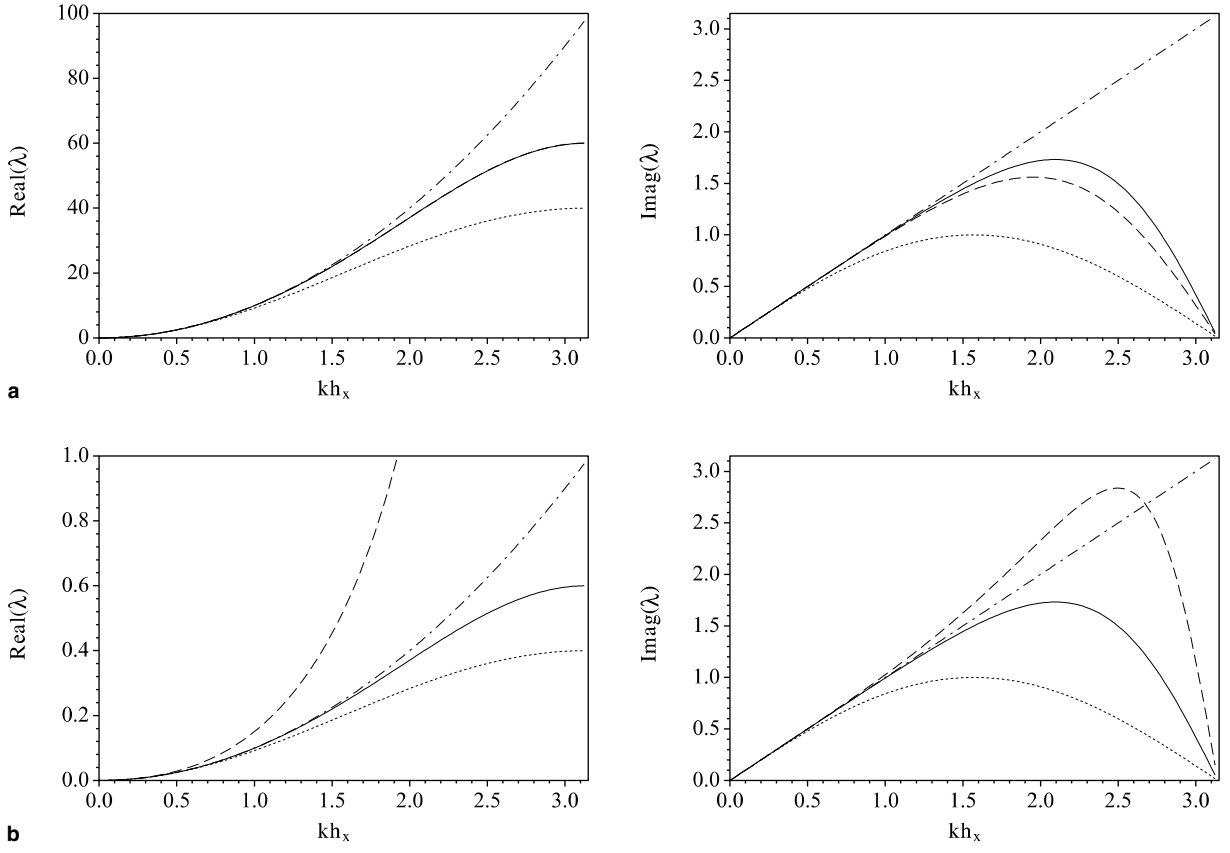

Fig. 1. Real and imaginary parts of λ for three numerical schemes: (a) $Pe = 0.1$ and (b) $Pe = 10$. ——, PDE; - - - -, HOC; ……., CD; -·-·-·-·-·-, exact.

$$\left(1+\frac{\Delta t}{2}c^x\frac{\partial}{\partial x}\right)\left(1-\frac{\Delta t}{2}v^x\frac{\partial^2}{\partial x^2}\right)\left(1+\frac{\Delta t}{2}c^y\frac{\partial}{\partial y}\right)\left(1-\frac{\Delta t}{2}v^y\frac{\partial^2}{\partial y^2}\right)\phi^{n+1}$$
$$=\left(1-\frac{\Delta t}{2}c^x\frac{\partial}{\partial x}\right)\left(1+\frac{\Delta t}{2}v^x\frac{\partial^2}{\partial x^2}\right)\left(1-\frac{\Delta t}{2}c^y\frac{\partial}{\partial y}\right)\left(1+\frac{\Delta t}{2}v^y\frac{\partial^2}{\partial y^2}\right)\phi^n+\mathcal{O}(\Delta t^2), \tag{8}$$

where the spatial derivative terms are approximated with the standard fourth-order Padé schemes. For instance, the first and second derivatives in x-direction are approximated as

$$\phi'_{i-1,j}+4\phi'_{i,j}+\phi'_{i+1,j}=-\frac{3}{h}\left(\phi_{i-1,j}-\phi_{i+1,j}\right), \tag{9}$$

$$\phi''_{i-1,j}+10\phi''_{i,j}+\phi''_{i+1,j}=\frac{12}{h^2}\left(\phi_{i-1,j}-2\phi_{i,j}+\phi_{i+1,j}\right) \tag{10}$$

or in matrix–vector notations,

$$\begin{aligned} L_x\Phi_{,x}&=A_x\Phi,\\ L_{xx}\Phi_{,xx}&=B_{xx}\Phi. \end{aligned} \tag{11}$$

The same approximations are also applied to the spatial derivative terms in y-direction.

In matrix–vector notation, Eq. (8) becomes

$$L_x^{-1}T_x^+L_{xx}^{-1}T_{xx}^-L_y^{-1}T_y^+L_{yy}^{-1}T_{yy}^-\Phi^{n+1}=L_x^{-1}T_x^-L_{xx}^{-1}T_{xx}^+L_y^{-1}T_y^-L_{yy}^{-1}T_{yy}^+\Phi^n, \tag{12}$$

where

$$T_x^{\pm} = \left(L_x \pm \frac{\Delta t}{2} c^x A_x\right), \quad T_{xx}^{\pm} = \left(L_{xx} \pm \frac{\Delta t}{2} v^x B_{xx}\right),$$
$$T_y^{\pm} = \left(L_y \pm \frac{\Delta t}{2} c^y A_y\right), \quad T_{yy}^{\pm} = \left(L_{yy} \pm \frac{\Delta t}{2} v^y B_{yy}\right). \tag{13}$$

The solution procedure only consists of a number of multiplications and inversions of tridiagonal matrices, and this makes the computation efficient compared to other non-ADI-based schemes [3,6] which require iterative methods for solving banded sparse matrices (also see [2] for the comparison of computational costs for ADI and non-ADI-based schemes). From Eqs. (9)–(11) and (13), it can be easily shown that $T^{+}_{x(y)}$ and $T^{-}_{xx(yy)}$ are non-singular tridiagonal matrices.

The present factorization retains the wave number characteristics discussed in Fig. 1 with $\mathcal{O}(\Delta t^2)$ accuracy. Consider subsets of the factored Eqs. (2) and (8)

$$\left(1 + \frac{\Delta t}{2}\left(c^x \frac{\partial}{\partial x} - v^x \frac{\partial^2}{\partial x^2}\right)\right)\phi = g \tag{14}$$

and

$$\left(1 + \frac{\Delta t}{2} c^x \frac{\partial}{\partial x}\right)\left(1 - \frac{\Delta t}{2} v^x \frac{\partial^2}{\partial x^2}\right)\phi = g. \tag{15}$$

It can be easily shown that modified wave number spectrums for Eqs. (14) and (15) are equivalent by second-order temporal accuracy:

$$\left(1 + \frac{\Delta t}{2} \mathrm{i} c^x \hat{k}^1 + \frac{\Delta t}{2} v^x \hat{k}^2\right) = \left(1 + \frac{\Delta t}{2} \mathrm{i} c^x \hat{k}^1\right)\left(1 + \frac{\Delta t}{2} v^x \hat{k}^2\right) + \mathcal{O}(\Delta t^2). \tag{16}$$

The von Neumann stability analysis is performed to examine the stability of the scheme. By assuming $\phi_{ij}^n = \phi_0^n \mathrm{e}^{\mathrm{i}k^x h_x} \mathrm{e}^{\mathrm{i}k^y h_y}$, we obtain the amplification factor σ in the following form:

$$\sigma = \frac{(1 - \mathrm{i}\alpha^x)(1 - \beta^x)}{(1 + \mathrm{i}\alpha^x)(1 + \beta^x)} \frac{(1 - \mathrm{i}\alpha^y)(1 - \beta^y)}{(1 + \mathrm{i}\alpha^y)(1 + \beta^y)}, \tag{17}$$

where

$$\alpha^{x(y)} = \frac{\Delta t}{2} c^{x(y)} \frac{3\sin(k^{x(y)} h_{x(y)})}{h_{x(y)}(2 + \cos(k^{x(y)} h_{x(y)}))},$$
$$\beta^{x(y)} = \frac{\Delta t}{2} v^{x(y)} \frac{12(1 - \cos(k^{x(y)} h_{x(y)}))}{h_{x(y)}^2(\cos(k^{x(y)} h_{x(y)}) + 5)}. \tag{18}$$

It can be easily shown that the criterion $|\sigma| \leqslant 1$ is satisfied for all $\alpha^{x(y)}$, $\beta^{x(y)}$. Therefore, the new scheme is unconditionally stable.

Extension of the present ADI method to a three-dimensional problem and a system of equations can be made as the same way for PR-ADI [1] or HOC-ADI [2] methods except for the additional factorization in the advection and diffusion steps. Stability and convergence of the present ADI method for linear and nonlinear systems of equations can be proved by applying the same approach used for PR-ADI method [17]. To demonstrate the potential of the present Padé-ADI method for three-dimensional nonlinear systems, a formulation for the incompressible Navier–Stokes equations are presented in Appendix A.

Forward or backward differences can be employed to impose Dirichlet, Neumann, or Robin type boundary conditions retaining the bandwidth and the strict diagonal dominancy of the matrices [1,2,4]. Mattsson and Nordström [18] showed that two and one orders less accurate boundary closures for the second and first derivatives terms, respectively, can maintain the internal order of accuracy. It is also worth noting that a strong stability of the present ADI scheme for non-periodic boundary conditions can be achieved by employing

the simultaneous approximation term (SAT) procedure [19,20]. The SAT procedure is a penalty method, where the penalty parameters are determined by stability considerations (see [18–22] for details).

3. Numerical examples

To examine the validity and effectiveness of the present high-order Padé ADI method, an unsteady problem concerning the convection–diffusion of a Gaussian pulse in the square domain $[0,2]\times[0,2]$ is considered with the following initial condition [2]:

$$\phi(0,x,y) = \exp\left(-\frac{(x-0.5)^2}{v^x} - \frac{(y-0.5)^2}{v^y}\right). \tag{19}$$

An analytical solution to this problem is

$$\phi(t,x,y) = \frac{1}{4t+1}\exp\left(-\frac{(x-c^x t-0.5)^2}{v^x(4t+1)} - \frac{(y-c^y t-0.5)^2}{v^y(4t+1)}\right). \tag{20}$$

The Dirichlet boundary conditions are taken from the analytical solution.

A uniform grid of $h_x = h_y = 0.025$ is employed to compare the accuracy of the computed solutions from the present Padé-ADI, the HOC-ADI, and the PR-ADI schemes. The viscosity values are fixed at $v^x = v^y = 0.01$. Two cell Reynolds numbers of $Pe = 2$ and 200 are considered by setting convection velocities $c^x = c^y = 0.8$ and $c^x = c^y = 80$. Constant times step sizes of 2.5×10^{-3} and 2.5×10^{-5} are used for $Pe = 2$ and 200, respectively.

Fig. 2 shows L^2-norm errors of the computed solutions at $Pe = 2$ with respect to the exact solution at each time step. The present ADI scheme produces a significantly more accurate solution than other schemes compared. Less accurate predictions of the HOC-ADI scheme are mainly due to phase errors as expected through the modified wave number study (see Fig. 1(a)). The PR-ADI method shows significantly higher magnitudes of L^2-norm errors. In [2], in this case, it was shown that the PR-ADI method cannot achieve the same order of L^2-norm errors of the HOC-ADI scheme even with twice the grid resolution. Numerical solutions are compared with the exact solution at the final time step ($t = 1.25$) in Fig. 3. Solutions obtained from the present ADI (Fig. 3(b)) and the HOC-ADI (Fig. 3(c)) schemes are visually indistinguishable from the exact solution (Fig. 3(a)). However, noticeable phase differences are observed between the PR-ADI solution (Fig. 3(d)) and the exact solution.

The superiority of the present ADI scheme is more clearly observed in the high cell Reynolds number case ($Pe = 200$). Fig. 4 shows contour plots of the numerical and exact solutions at $t = 0.0125$. The present ADI scheme produces a solution in good agreement with the exact solution in terms of amplitude and phase

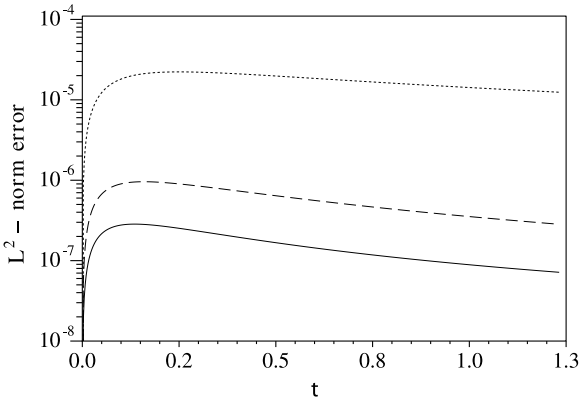

Fig. 2. L^2-norm errors produced by three numerical schemes at each time step: ——, present ADI scheme; - - - -, HOC-ADI scheme [2]; ……., PR-ADI scheme [1]. $\Delta t = 0.0025$, $\Delta x = \Delta y = 0.025$, $c^x = c^y = 0.8$ and $v^x = v^y = 0.01$.

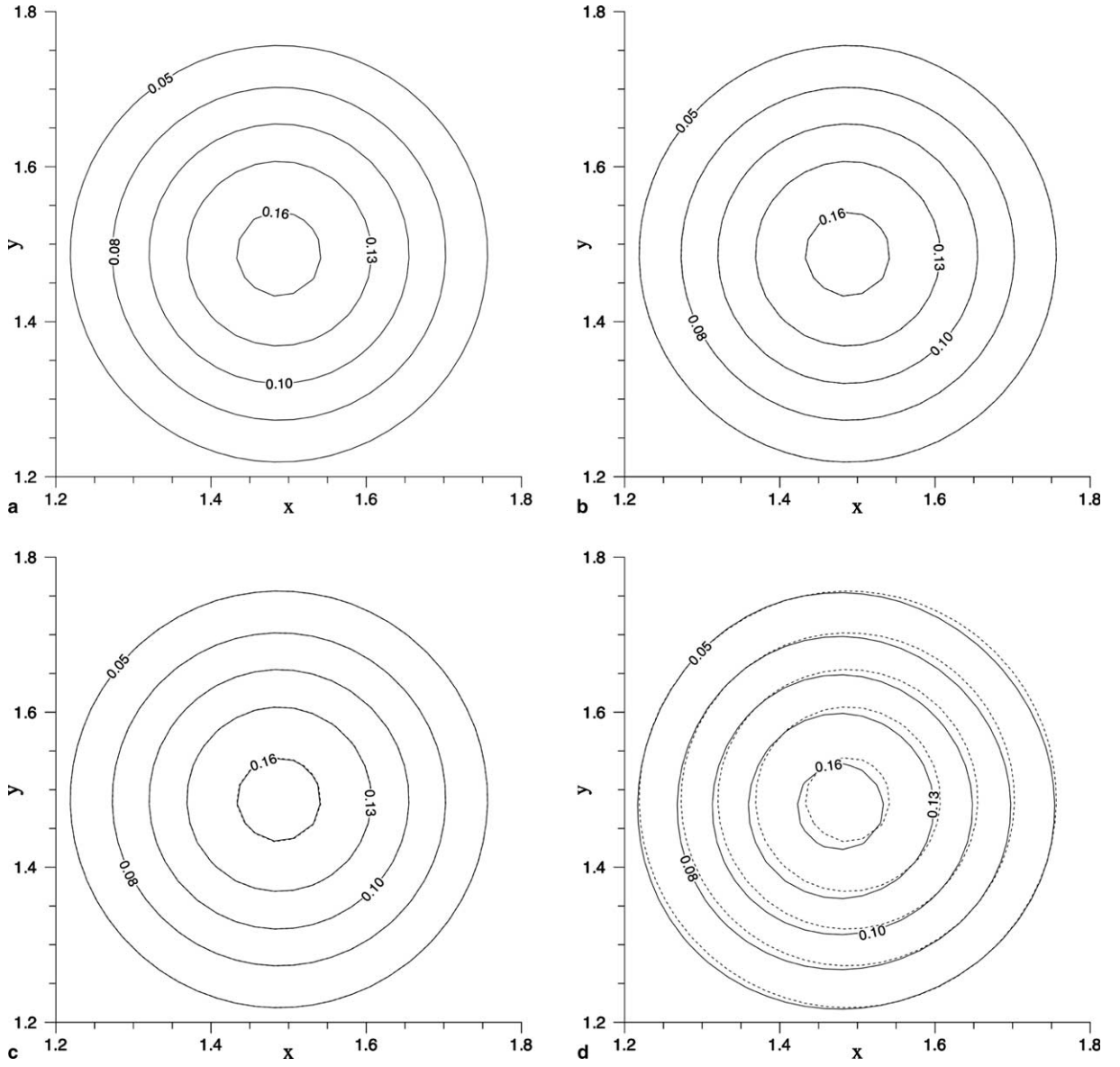

Fig. 3. Contour plots of the pulse in the region $1.2 \leqslant x, y \leqslant 1.8$ at $t = 1.25$: (a) exact, (b) present ADI, (c) HOC-ADI [2], and (d) PR-ADI [1]. $\Delta t = 2.5 \times 10^{-3}$, $\Delta x = \Delta y = 0.025$, $c^x = c^y = 0.8$ and $v^x = v^y = 0.01$. Dotted contour lines in (b)–(d) correspond to the exact solution.

(Fig. 4(a) and (b)). However, the HOC-ADI scheme and the PR-ADI scheme lead to significantly dissipated solutions which are also highly distorted and oscillatory (Fig. 4(c) and (d)). In particular, the enhanced numerical dissipation makes the HOC-ADI scheme unattractive for direct numerical simulations or large eddy simulations of turbulent flows. The distortions and oscillations are in opposite-direction in the solution of HOC-ADI and PR-ADI schemes, and this feature is explained by the characteristics of the imaginary parts of the λs for a high cell Reynolds number case (see Fig. 1(b)).

At $Pe = 200$, the three numerical schemes are compared quantitatively in Table 1. The present ADI scheme shows a much smaller L^2-norm error than those of other ADI schemes. However, in contrast to the case of $Pe = 2$, the L^2-norm error of the HOC-ADI scheme is not significantly lower than that of the PR-ADI method. A disadvantage of the present ADI scheme is the higher computational cost due to the increased

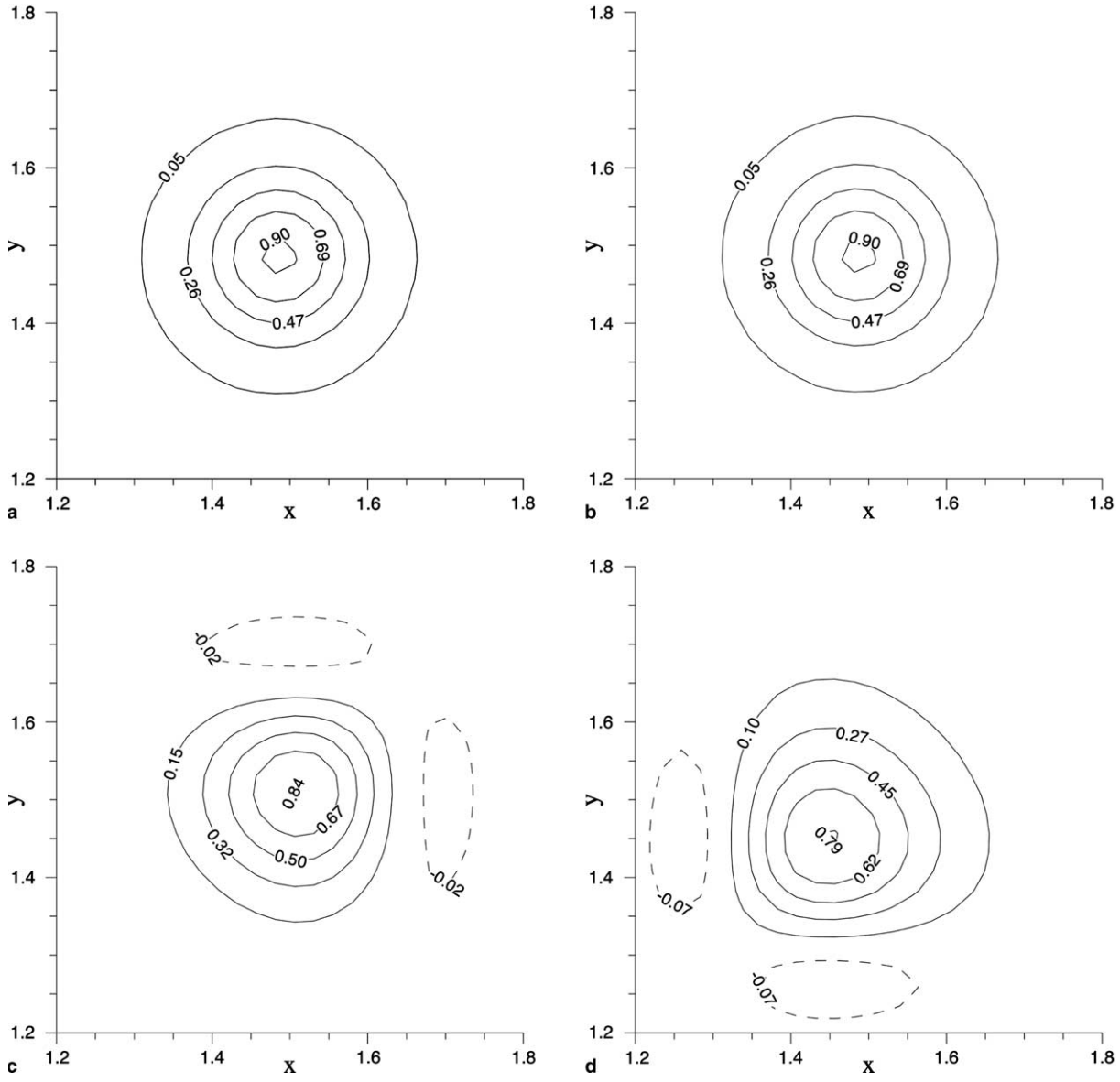

Fig. 4. Contour plots of the pulse in the region $1.2 \leqslant x, y \leqslant 1.8$ at $t = 0.0125$: (a) exact, (b) present ADI, (c) HOC-ADI [2], and (d) PR-ADI [1]. $\Delta t = 2.5 \times 10^{-5}$, $\Delta x = \Delta y = 0.025$, $c^x = c^y = 80$ and $v^x = v^y = 0.01$.

number of factorizations of the governing equation. However, it is worth noting that, at this high cell Reynolds number, the present scheme produces better results than the HOC-ADI scheme employing the double mesh size.

Table 1
L^2-norm errors at $t = 0.0125$ and CPU times used for numerical integrations

Scheme	L^2-norm error	$\frac{\text{CPU time}}{\text{CPU time for PR-ADI}}$
PR-ADI [1]	3.29×10^{-4}	1.0
HOC-ADI [2]	1.82×10^{-4}	1.4
Present ADI	7.68×10^{-6}	2.2

$\Delta t = 2.5 \times 10^{-5}$, $\Delta x = \Delta y = 0.025$, $c^x = c^y = 80$ and $v^x = v^y = 0.01$.

4. Concluding remarks

A high-order alternating direction implicit (ADI) method for computation of unsteady convection–diffusion equations has been proposed. The Padé approximations of spatial derivatives lead to fourth-order accuracy with high resolution properties in space, while second-order accuracy is maintained in time. The solution procedure consists of a number of multiplications and inversions of tridiagonal matrices which are computationally cost effective. The present method is unconditionally stable and produces more accurate solutions in terms of phase and amplitude errors than the standard second-order ADI method [1] and the fourth-order HOC-ADI scheme [2]. In particular, it does not introduce numerical dissipation which is significant in the convection-dominated case when other previous ADI schemes are employed.

Acknowledgements

The author acknowledges the support of the Office of Naval Research under Grant No. N00014-99-1-0389. Fruitful comments of Dr. Meng Wang on a draft of this note are greatly appreciated.

Appendix A. Padé ADI method for incompressible Navier–Stokes equations

Consider the incompressible Navier–Stokes equations in the conservative form:

$$\begin{aligned}&\frac{\partial u_i}{\partial t} = -\frac{\partial}{\partial x_j}u_i u_j + \frac{1}{Re}\frac{\partial^2}{\partial x_j \partial x_j}u_i - \frac{\partial p}{\partial x_i},\\ &\frac{\partial u_i}{\partial x_i} = 0.\end{aligned} \tag{A.1}$$

Applying the Crank–Nicolson scheme and the fractional-step method [23] to Eq. (A.1) leads to

$$\frac{\hat{u}_i - u_i^n}{\Delta t/2} = -\left(\frac{\delta}{\delta x_j}\hat{u}_i\hat{u}_j - \frac{1}{Re}\frac{\delta^2}{\delta x_j \delta x_j}\hat{u}_i\right) - \left(\frac{\delta}{\delta x_j}u_i^n u_j^n - \frac{1}{Re}\frac{\delta^2}{\delta x_j \delta x_j}u_i^n\right), \tag{A.2}$$

$$\frac{u_i^{n+1} - \hat{u}_i}{\Delta t} = -\frac{\delta \phi^{n+1}}{\delta x_i}, \tag{A.3}$$

$$\frac{\delta u_i^{n+1}}{\delta x_i} = 0, \tag{A.4}$$

where ϕ is referred to as the pseudo-pressure and is different from the original pressure p by

$$\frac{\delta p^{n+1}}{\delta x_i} = \frac{\delta \phi^{n+1}}{\delta x_i} + \mathcal{O}(\Delta t). \tag{A.5}$$

Eq. (A.2) can be recast as

$$\hat{u}_i + \frac{\Delta t}{2}\left(\frac{\delta}{\delta x_j}\hat{u}_i\hat{u}_j - \frac{1}{Re}\frac{\delta^2}{\delta x_j \delta x_j}\hat{u}_i\right) = u_i^n - \frac{\Delta t}{2}\left(\frac{\delta}{\delta x_j}u_i^n u_j^n - \frac{1}{Re}\frac{\delta^2}{\delta x_j \delta x_j}u_i^n\right) \equiv R_i^n \tag{A.6}$$

or

$$F_i = \hat{u}_i + \frac{\Delta t}{2}\left(\frac{\delta}{\delta x_j}\hat{u}_i\hat{u}_j - \frac{1}{Re}\frac{\delta^2}{\delta x_j \delta x_j}\hat{u}_i\right) - R_i^n = 0. \tag{A.7}$$

Applying a Newton-iteration method to Eq. (A.7) leads to

$$\left\{\frac{\partial F_i}{\partial \hat{u}_j}\right\}^r \delta\hat{u}_j^{r+1} = -F_i^r, \tag{A.8}$$

where $\delta\hat{u}_j^{r+1} = \hat{u}_j^{r+1} - \hat{u}_j^r$, r is the iteration index, and $j = 1, 2, 3$. Then

$$\left\{\delta_{ij}+\frac{\Delta t}{2}\frac{\partial}{\partial\hat{u}_j}\left(\frac{\delta}{\delta x_j}\hat{u}_i\hat{u}_j-\frac{1}{Re}\frac{\delta^2}{\delta x_j\delta x_j}\hat{u}_i\right)\right\}^r\delta\hat{u}_j^{r+1}=-F_i^r, \tag{A.9}$$

and we introduce a matrix of the form

$$M_{ij}=\left\{\frac{\partial}{\partial\hat{u}_j}\left(\frac{\delta}{\delta x_j}\hat{u}_i\hat{u}_j-\frac{1}{Re}\frac{\delta^2}{\delta x_j\delta x_j}\hat{u}_i\right)\right\}. \tag{A.10}$$

Now we split $M_{ij}=(M_{ij}^1+M_{ij}^2+M_{ij}^3)$ into three parts each containing x_1, x_2 and x_3-derivatives, respectively. Using an ADI factorization technique, Eq. (A.9) becomes

$$\left(1+\frac{\Delta t}{2}M_{ii}^1\right)^r\left(1+\frac{\Delta t}{2}M_{ii}^2\right)^r\left(1+\frac{\Delta t}{2}M_{ii}^3\right)^r\delta\hat{u}_i^{r+1}=-F_i^r-\kappa\frac{\Delta t}{2}(M_{ij})^r\delta\hat{u}_j^*, \tag{A.11}$$

where $\kappa=1$ for $j\neq i$ and $\kappa=0$ for $j=i$ with $j=1,2,3$. No summation rule is repeated on $i\,(=1,2,3)$. $\delta\hat{u}_j^*$ is updated during the iteration step. The factored terms in the left-hand side of Eq. (A.11) become tridiagonal matrices when the spatial derivatives are approximated by the second-order central differences. Inversions of the tridiagonal matrices result in a significant reduction in computing cost and memory. This formulation has been successfully employed in a number of direct- and large-eddy simulations of turbulent flows [11–13].

Interestingly, Visbal and Gaitonde [14] employed second-order central differences and fourth-order Padé schemes for the spatial derivative terms in the left- and right-hand sides of Eq. (A.11) to obtain global high-order spatial accuracy. Second-order central differences for the factored terms were necessary to retain the efficiency of tridiagonal matrix operations. The present ADI method allows the use of fourth-order Padé schemes for the left-hand side factored terms maintaining the efficiency of tridiagonal matrix operations. Applicability of the present ADI method is considered for the case of i = 1 as:

$$\begin{aligned}&\left(1+\frac{\Delta t}{2}\frac{\delta}{\delta x_1}2\hat{u}_1\right)^r\left(1-\frac{\Delta t}{2}\frac{1}{Re}\frac{\delta^2}{\delta x_1\delta x_1}\right)^r\left(1+\frac{\Delta t}{2}\frac{\delta}{\delta x_2}\hat{u}_2\right)^r\left(1-\frac{\Delta t}{2}\frac{1}{Re}\frac{\delta^2}{\delta x_2\delta x_2}\right)^r\\&\quad\cdot\left(1+\frac{\Delta t}{2}\frac{\delta}{\delta x_3}\hat{u}_3\right)^r\left(1-\frac{\Delta t}{2}\frac{1}{Re}\frac{\delta^2}{\delta x_3\delta x_3}\right)^r\delta\hat{u}_1^{r+1}=-F_1^r-\frac{\Delta t}{2}\frac{\delta}{\delta x_2}(\hat{u}_1\delta\hat{u}_2^*)-\frac{\Delta t}{2}\frac{\delta}{\delta x_3}(\hat{u}_1\delta\hat{u}_3^*),\end{aligned} \tag{A.12}$$

where

$$\begin{aligned}M_{11}^1\delta\hat{u}_1&=\frac{\delta}{\delta x_1}(2\hat{u}_1\delta\hat{u}_1)-\frac{1}{Re}\frac{\delta^2}{\delta x_1\delta x_1}\delta\hat{u}_1,\\M_{11}^2\delta\hat{u}_1&=\frac{\delta}{\delta x_2}(\hat{u}_2\delta\hat{u}_1)-\frac{1}{Re}\frac{\delta^2}{\delta x_2\delta x_2}\delta\hat{u}_1,\\M_{11}^3\delta\hat{u}_1&=\frac{\delta}{\delta x_3}(\hat{u}_3\delta\hat{u}_1)-\frac{1}{Re}\frac{\delta^2}{\delta x_3\delta x_3}\delta\hat{u}_1,\\M_{12}\delta\hat{u}_2&=\frac{\delta}{\delta x_2}(\hat{u}_1\delta\hat{u}_2),\\M_{13}\delta\hat{u}_3&=\frac{\delta}{\delta x_3}(\hat{u}_1\delta\hat{u}_3).\end{aligned} \tag{A.13}$$

References

[1] D.W. Peaceman, H.H. Rachford Jr., The numerical solution of parabolic and elliptic differential equations, Journal of the Society of Industrial and Applied Mathematics 3 (1959) 28–41.
[2] S. Karaa, J. Zhang, High order ADI method for solving unsteady convection–diffusion problems, Journal of Computational Physics 198 (2004) 1–9.
[3] J.C. Kalita, D.C. Dalal, A.K. Dass, A class of higher order compact schemes for the unsteady two-dimensional convection–diffusion equation with variable convection coefficients, International Journal for Numerical Methods in Fluids 38 (2002) 1111–1131.
[4] W.F. Spotz, G.F. Carey, Extension of high-order compact schemes to time-dependent problems, Numerical Methods for Partial Differential Equations 17 (2001) 657–672.

[5] A. Rigal, High order difference schemes for unsteady one-dimensional diffusion–convection problems, Journal of Computational Physics 114 (1994) 59–76.
[6] B.J. Noye, H.H. Tan, Finite difference methods for solving the two-dimensional advection–diffusion equation, International Journal for Numerical Methods in Fluids 26 (1988) 1615–1629.
[7] P.J. van der Houwen, H.B. de Vries, Fourth order ADI method for semidiscrete parabolic equations, Journal of Computational and Applied Mathematics 9 (1) (1983) 41–63.
[8] H.B. de Vries, Comparative study of ADI splitting methods for parabolic equations in two space dimensions, Journal of Computational and Applied Mathematics 10 (2) (1984) 179–193.
[9] P.J. van der Houwen, Iterated splitting methods of high order for time-dependent partial differential equations, SIAM Journal on Numerical Analysis 21 (4) (1984) 635–656.
[10] R.J. MacKinnon, G.F. Carey, Analysis of material interface discontinuities and superconvergent fluxes in finite difference theory, Journal of Computational Physics 75 (1988) 151–167.
[11] H. Choi, P. Moin, J. Kim, Turbulent drag reduction: studies of feedback control and flow over riblets, Report TF-55, Department of Mechanical Engineering, Stanford University, Stanford, California, September 1992.
[12] K. Akselvoll, P. Moin, Large eddy simulation of turbulent confined coannular jets and turbulent flow over a backward facing step, Report TF-63, Department of Mechanical Engineering, Stanford University, Stanford, California, February 1995.
[13] D. You, R. Mittal, M. Wang, P. Moin, Computational methodology for large-eddy simulation of tip-clearance flows, AIAA Journal 42 (2) (2004) 271–279.
[14] M.R. Visbal, D.V. Gaitonde, High-order-accurate methods for complex unsteady subsonic flows, AIAA Journal 37 (10) (1999) 1231–1239.
[15] R. Mittal, P. Moin, Suitability of upwind-biased schemes for large-eddy simulation of turbulent flows, AIAA Journal 36 (1997) 1415–1417.
[16] P. Moin, Fundamentals of Engineering Numerical Analysis, Cambridge University Press, 2001.
[17] W.H. Hundsdorfer, J.G. Verwer, Stability and convergence of the Peaceman–Rachford ADI method for initial-boundary value problems, Mathematics of Computation 53 (187) (1989) 81–101.
[18] K. Mattsson, J. Nordström, Summation by parts operators for finite difference approximations of second derivatives, Journal of Computational Physics 199 (2004) 503–540.
[19] M.H. Carpenter, D. Gottlieb, S. Abarbanel, Time-stable boundary conditions for finite-difference schemes solving hyperbolic systems: methodology and application to high-order compact schemes, Journal of Computational Physics 111 (1994) 220–236.
[20] K. Mattsson, Private communication, 2005.
[21] B. Strand, Summation by parts for finite difference approximations for d/dx, Journal of Computational Physics 110 (1994) 47–67.
[22] M.H. Carpenter, J. Nordström, D. Gottlieb, A stable conservative interface treatment of arbitrary spatial accuracy, Journal of Computational Physics 148 (1999) 341–365.
[23] J. Kim, P. Moin, Application of a fractional-step method to incompressible Navier–Stokes equations, Journal of Computational Physics 59 (1985) 308–323.